APPLIED ORGANOMETALLIC CHEMISTRY
Appl. Organometal. Chem. 2006; **20**: 220–225
Published online 19 December 2005 in Wiley InterScience (www.interscience.wiley.com). DOI:10.1002/aoc.1030

Triphenyltin hydroxide as a precursor for the synthesis of nanosized tin-doped TiO_2 photocatalysts

Fernando Fresno[1,2], David Tudela[1]*, A. Javier Maira[2], Francisco Rivera[1], Juan M. Coronado[3] and Javier Soria[2]

[1]Departamento de Química Inorgánica, Facultad de Ciencias, Universidad Autónoma de Madrid, 28049 Madrid, Spain
[2]Instituto de Catálisis y Petroleoquímica, CSIC, c/Marie Curie 2, Cantoblanco, 28049 Madrid, Spain
[3]Laboratorio de Aplicaciones Medioambientales de la Energía Solar, CIEMAT, Av. Complutense 22, 28040 Madrid, Spain

Received 16 October 2005; Revised 5 November 2005; Accepted 7 November 2005

^{1}H and ^{119}Sn NMR results indicate that, when Ph_3SnOH is dissolved in CD_2Cl_2, it dehydrates to $(Ph_3Sn)_2O$, only a small amount of Ph_3SnOH remaining in equilibrium at room temperature. As a result, the reaction of $TiCl_4$ with Ph_3SnOH in CH_2Cl_2 proceeds via hydrolysis of the halide to precipitate amorphous TiO_2 that contains adsorbed organotin species. Calcination of the amorphous precursor to 723 K yields nanoparticles of tin-doped TiO_2 photocatalysts, that contain anatase and rutile phases, and may also contain a segregated SnO_2 phase. The reaction conditions that lead to the formation of a SnO_2 phase have been studied and we have found that it is formed when the amorphous precipitate is not thoroughly washed with CH_2Cl_2 or when non-recrystallized commercial Ph_3SnOH is used as a starting material. The catalysts obtained have a high activity for the photooxidation of toluene in the gas phase. In particular, a material obtained from non-recrystallized Ph_3SnOH is particularly promising because the toluene photooxidation rate is more than twice as high as when using Degussa P25. Copyright © 2005 John Wiley & Sons, Ltd.

KEYWORDS: organotin; ^{119}Sn; TiO_2; SnO_2; anatase; rutile; photocatalysis; tin-doped; nanoparticles; toluene

INTRODUCTION

Trimethyltin fluoride has been widely used by Roesky's group for the preparation of metallic and organometallic fluorides by means of halide metathesis reactions.[1–3] Bearing in mind that triorganotin hydroxides are isoelectronic with the corresponding fluorides, they could give rise to similar nucleophilic substitution reactions leading to metallic hydroxides. Indeed, three decades ago, Zuckerman prepared $Sn(OH)_2$ by reaction of $SnCl_2$ with triphenyl- and trimethyl-tin hydroxide,[4] and later DuMont used a similar reaction to transform $M(CO)_5SnCl_2 \cdot THF$ (M = Cr, W) into $M(CO)_5Sn(OH)_2$.[5] Hydroxide exchange has also been observed in the reaction between Me_3Al and Ph_3SnOH.[6] Because of the high polarizing power of cations in high oxidation state, their hydroxides are expected to dehydrate spontaneously to the corresponding oxides, and the reaction of $TiCl_4$ with Ph_3SnOH in organic solvents was expected to proceed according to the following equation:

$$TiCl_4 + 4\ Ph_3SnOH \longrightarrow TiO_2 + 2H_2O + 4\ Ph_3SnCl \quad (1)$$

It is known that Ph_3SnCl adsorbs on the TiO_2 surface,[7] and adsorption should be enhanced for small amorphous TiO_2 particles precipitating from an organic solution with a high content of triphenyltin compounds. Accordingly, reaction (1) in CH_2Cl_2 leads to amorphous TiO_2 with adsorbed organotin compounds which give rise to nanosized $Ti_{1-x}Sn_xO_2$ crystalline materials by thermal or hydrothermal treatments.[8,9]

Heterogeneous photocatalysis is an efficient technique for the elimination of organic pollutants, both in aqueous solution and in the gas phase, and titanium dioxide is the most widely used photocatalyst because of its relatively high photoactivity, its stability under operation conditions and its low cost and toxicity.[10,11] The anatase phase generally has much higher photocatalytic activity than rutile, but anatase/rutile contacts may increase the activity, as in

*Correspondence to: David Tudela, Departamento de Química Inorgánica, Universidad Autónoma de Madrid, 28049 Madrid, Spain.
E-mail: David.tudela@uam.es
Contract/grant sponsor: Spanish Ministerio de Educación y Ciencia;
Contract/grant number: CTQ2004-03409/BQU.

the case of P25 (Degussa) which is often considered as a benchmark in photocatalysis.[12] Among the different approaches to improve the photoactivity of TiO_2, there is current interest in the SnO_2–TiO_2 system[12–21] and in tin-doped TiO_2 materials.[8,9,22–24] The nanocrystalline samples obtained by calcination of the amorphous precipitate obtained in reaction (1) contain the anatase and rutile TiO_2 phases and show a high activity for the photocatalytic oxidation of methylcyclohexane in the gas phase.[8] Nevertheless, some of the prepared samples contained an SnO_2 (cassiterite) phase, in addition to anatase and rutile, and showed a reduced activity for the photocatalytic degradation of chlorsulfuron, a sulfonylurea herbicide, in aqueous solution.[9] Therefore, it is important to control the factors that lead to the appearance of a SnO_2 phase in the $Ti_{1-x}Sn_xO_2$ photocatalysts obtained by means of reaction (1).

Another factor concerning the mechanism of reaction (1) is the integrity of Ph_3SnOH in CH_2Cl_2 solution, because triorganotin hydroxides and oxides may exist in equilibrium.[25] Although reports on the solution ^{119}Sn NMR spectra of Ph_3SnOH do not talk about dehydration, the reported chemical shift data in non-coordinating solvents (between −82.5 and −86 ppm)[26,27] are very close to those reported for $(Ph_3Sn)_2O$ (between −83.1 and −85.5 ppm).[28–30] In this work, we have studied the ^{119}Sn NMR spectra of Ph_3SnOH in CD_2Cl_2 solution at different temperatures and gained insight into the mechanism of reaction (1). In addition, we have checked the factors that influence the segregation of a SnO_2 phase in the obtained $Ti_{1-x}Sn_xO_2$ crystalline materials and studied their catalytic activity for the photocatalytic oxidation of toluene into CO_2 and water in the gas phase. Toluene was selected because it is thought to be an important constituent of emissions in urban atmospheres and the photocatalytic oxidation of aromatic compounds is slow in comparison to other organic compounds, so that better catalysts are required for the degradation of this kind of pollutants.[31,32]

EXPERIMENTAL

Synthesis of the photocatalysts

Triphenyltin hydroxide (Aldrich) was recrystallized from distilled 96% ethanol and the crystalline colorless needles were characterized by IR spectroscopy.[33] The insoluble residue of the recrystallization was washed several times with ethanol and characterized essentially as Ph_2SnO by Raman spectroscopy and elemental analysis. For the synthesis of the tin doped TiO_2 photocatalysts, both recrystallized and non-recrystallized Ph_3SnOH samples were used. In a typical preparation, a solution containing 120 mmol of Ph_3SnOH in 380 ml of dry CH_2Cl_2 was prepared by refluxing the mixture under an argon atmosphere (while clear solutions were obtained for recrystallized Ph_3SnOH, some turbidity was observed for the non-recrystallized samples). After cooling to room temperature, a solution of 27.3 mmols of $TiCl_4$ (Aldrich) in 10 ml of dry CH_2Cl_2 was added drop by drop, under argon, to the stirred organotin solution, and a white precipitate appeared immediately. The mixture was stirred at room temperature for 16 h and the solid was filtered off, washed with six portions of CH_2Cl_2, dried in air and ground in an agate mortar. The white amorphous powder was calcined in air at 723 K for 3 h, yielding the nanocrystalline materials. Evaporation of the CH_2Cl_2 filtrate yielded almost the theoretical amount of triphenyltin chloride that was characterized by IR spectroscopy.[33,34] TiSnT1 and TiSnA1 are representative samples when recrystallized and non-recrystallized Ph_3SnOH, respectively, are used in the above-described procedure. The sample of TiSnB1 was obtained when recrystallized Ph_3SnOH was used, but the amorphous white precipitate was not thoroughly washed with CH_2Cl_2.

Analytical methods and physical techniques

^{119}Sn NMR spectra were obtained with saturated CD_2Cl_2 solutions of Ph_3SnOH (ca 0.35 M at room temperature) with a Bruker DRX-500 (at 298 and 223 K) and a Bruker AMX-300 (at 198 K), operating at 186.48 and 111.91 MHz, respectively. ^{1}H NMR spectra were recorded at room temperature in CD_2Cl_2 solution on a Bruker AMX-300 spectrometer operated at 300.14 MHz. Chemical shifts are referenced to $SnMe_4$ for ^{119}Sn and $SiMe_4$ for ^{1}H. Infrared spectra were recorded on a Perkin-Elmer 1650 FT-IR instrument, using KBr pellets. Raman spectra were measured at room temperature on a Bruker RFS-100 FT-Raman instrument, using an Nd–Y–Ag laser (λ = 1064 nm), or a Renishaw Ramascope 2000 microspectrometer with an Ar laser (λ = 514.5 nm). The microanalyses (C, H and N) were carried out with a Perkin-Elmer 2400 CHN elemental analyzer. The tin content was determined by X-ray fluorescence, using a TXRF Extra-II Rich & Seifert instrument, or by ICP spectroscopy, in a Perkin-Elmer Optima 3300 DV equipment, selecting λ = 189.297 nm. The phase composition and particle size of the materials were characterized by powder X-ray diffraction using a Seifert XRD 3000P diffractometer and nickel-filtered Cu K_α radiation. The primary particle size was estimated from line-broadening by means of the Scherrer equation. The surface area (BET) of the materials was measured by nitrogen physisorption at 77 K in a Micromeritics 2100 apparatus.

Photocatalytic activity tests

The photocatalytic activity for the gas-phase oxidation of toluene was tested in a continuous flow annular photoreactor that has been described elsewhere.[31] The photoreactor was made of two concentric Pyrex tubes, and a slurry of the catalysts powder in ethanol was spread on the external surface of the inner glass tube, and dried at room temperature to form a relatively uniform coating. The reactant mixture was prepared by injecting ca. 700 ppmv of toluene (Panreac, 99%) with a syringe into a wet oxygen flow (ca. 75% relative humidity) that passed between the two tubes. The reactor was illuminated by four external UV lamps (Sylvania 6WBLB-T5, 6 W). Regular analyses of the outlet gas flow were carried

out by means of a Hewlett Packard GC-MS, using a HP-5 (0.25 mm × 30 m) capillary column and the SIM mode of the detector.

RESULTS AND DISCUSSION

Solution of Ph_3SnOH in CH_2Cl_2 and reaction with $TiCl_4$

The ^{119}Sn NMR data for saturated solutions of Ph_3SnOH in CD_2Cl_2 are shown in Table 1. At 298 K most of the tin-containing molecules (integral area 92%) are $(Ph_3Sn)_2O$, as demonstrated by the observation of ^{117}Sn satellites. The $^2J(^{119}Sn-^{119}Sn)$ coupling constant (423.4 Hz) is in the range reported for $(Ph_3Sn)_2O$ in other non-coordinating solvents (410.8–440.2 Hz),[28–30] and very close to that reported in the solid state (421 Hz).[35] The small signal at −87.1 ppm (integral area 8%) must correspond to Ph_3SnOH with a monomeric tetrahedral structure, in contrast to the polymeric penta-coordinated solid state structure, with bridging OH groups,[36,37] that give rise to $\delta_{iso} = -298$ ppm in the solid-state ^{119}Sn NMR spectrum.[38] The chemical shift of the molecules in equilibrium with Ph_3SnOH (−84.4 ppm) is in the range reported for $(Ph_3Sn)_2O$ in other non-coordinating solvents (between −83.1 and −85.5 ppm),[28–30] while solid-state spectra show two different tin signals, at δ_{iso} ca. −76 and −81 ppm,[35,39] in agreement with the two crystallographically independent tetra-coordinated tin atoms found in the crystal structure determination.[40] When the temperature is lowered to 223 and 198 K (see Table 1), the signal corresponding to Ph_3SnOH disappears, while the signal corresponding to $(Ph_3Sn)_2O$ shifts downfield and $^2J(^{119}Sn-^{119}Sn)$ decreases. This is consistent with a small decrease in the Sn–O–Sn angle as the temperature is lowered, according to the published correlation with $^2J(^{119}Sn-^{119}Sn)$.[39]

The ^1H NMR spectrum of CD_2Cl_2 (Aldrich) shows a small singlet at 1.52 ppm corresponding to dissolved water. When Ph_3SnOH is dissolved, the peak appears at 1.54 ppm and its intensity increases in ca. 1 H in relation to the 15 phenyl protons. In connection with the ^{119}Sn NMR results, it can be interpreted in terms of dehydration of Ph_3SnOH and fast exchange of the water protons with the OH of the small amount of Ph_3SnOH in equilibrium with $(Ph_3Sn)_2O$. Therefore, the ^1H and ^{119}Sn NMR results indicate that, when Ph_3SnOH is dissolved in CD_2Cl_2, it dehydrates according to equation (2), only a small amount of Ph_3SnOH remaining in equilibrium at room temperature.

$$4\ Ph_3SnOH \rightleftharpoons 2\ Ph_3SnOSnPh_3 + 2H_2O \qquad (2)$$

At 223 and 198 K, the water in the solvent freezes out so the equilibrium is completely shifted to the right. Old reports on the IR spectrum of Ph_3SnOH solutions in anhydrous CS_2 or CCl_4 also point to dehydration,[33,41] and equilibrium between the hydroxide and the oxide has also been detected for other triaryltin species.[42,43] Consistently with the dehydration of Ph_3SnOH when dissolved in CH_2Cl_2, we have found that the solid obtained by evaporation of Ph_3SnOH solutions in CH_2Cl_2 has an IR spectrum corresponding to $(Ph_3Sn)_2O$.[33] Therefore, reaction (1) does not proceed by direct hydroxide exchange but is the result of reactions (2)–(4), the hydrolysis of $TiCl_4$ [reaction (3)] being the origin of TiO_2:

$$TiCl_4 + 2H_2O \longrightarrow TiO_2 + 4\ HCl \qquad (3)$$

$$2\ Ph_3SnOSnPh_3 + 4\ HCl \longrightarrow 4\ Ph_3SnCl + 2H_2O \qquad (4)$$

The organotin compounds adsorbed on the surface of amorphous TiO_2 may be changing as the reactions proceed because initially there is a large amount of $(Ph_3Sn)_2O$ that later reacts with HCl according to equation (4), while at the end of the reaction, there is a large amount of Ph_3SnCl.

Table 1. ^{119}Sn NMR spectra of Ph_3SnOH in CD_2Cl_2 solution

T (°K)	Species	δ (ppm)	$^2J(^{119}Sn-^{119}Sn)$ (Hz)[a]
298	Ph_3SnOH	−87.1[b]	—
	$(Ph_3Sn)_2O$[c]	−84.4	423.4
223	$(Ph_3Sn)_2O$[c]	−80.9	389.7
198	$(Ph_3Sn)_2O$[c]	−79.3	378.1

[a] Obtained by multiplying $^2J(^{119}Sn-^{117}Sn)$ with $\gamma(^{119}Sn)/\gamma(^{117}Sn) = 1.0462$.
[b] Integral area 8%.
[c] $^1J(^{119}Sn-^{13}C)$ (ca. 626 Hz) does not show any significant temperature dependence.

Structural characteristics of the photocatalysts

The powder X-ray diffraction (XRD) patterns of the obtained photocatalysts are shown in Fig. 1 with those corresponding to the reference materials TiO_2 P25 and SnO_2. All three catalysts contain anatase and rutile, but TiSnA1 and TiSnB1 also contain a segregated SnO_2 phase. When non-recrystallized Ph_3SnOH was used as starting material, the XRD pattern of the final photocatalyst (TiSnA1) also shows small peaks corresponding to the (2 0 0) and (2 2 0) reflections of NaCl. This impurity comes from the commercial Ph_3SnOH, suggesting that is was prepared from Ph_3SnCl and NaOH, but not completely washed with water. The Raman spectra displayed in Fig. 2 show the peaks corresponding to anatase,[44] while the presence of rutile is hardly seen in the small shoulder at 609 cm^{-1} and the weak broad band at 443 cm^{-1},[44] and SnO_2 is not observed at all because its main features[44] are overlapped with stronger anatase peaks. The main structural characteristics of the prepared materials are summarized in Table 2. When we considered the factors contributing to the formation of a separate SnO_2 phase, we found that, every time that the reaction was carried out using recrystallized Ph_3SnOH and the amorphous white precipitate was thoroughly washed with CH_2Cl_2 as detailed in the experimental section, we obtained a material (represented by TiSnT1) that contained anatase and rutile but not a SnO_2

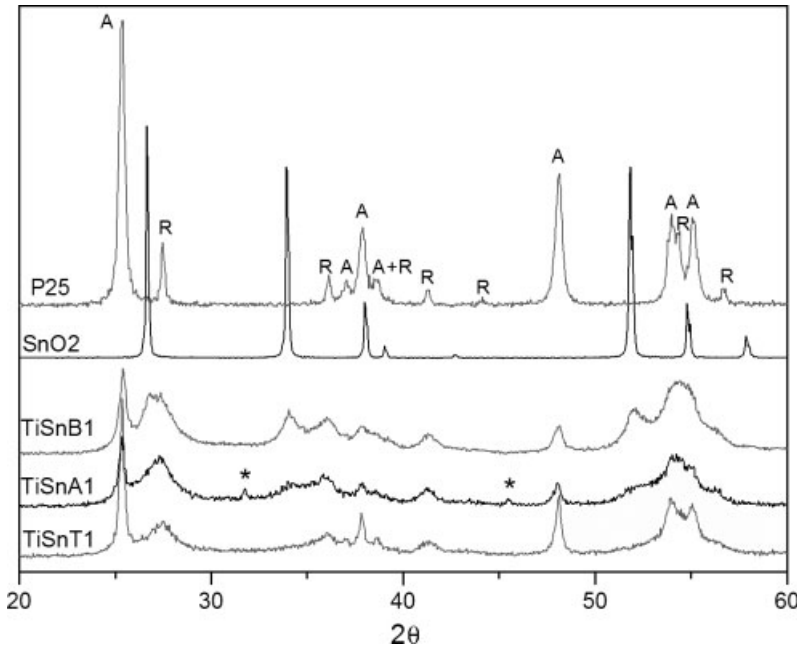

Figure 1. Powder X-ray diffraction patterns of P25 (Degussa), SnO_2 (Probus) and the obtained tin doped photocatalysts (A, anatase; R, rutile). Peaks due to NaCl, that appear when commercial non-recrystallized Ph_3SnOH is used (see text) are marked with an asterisk.

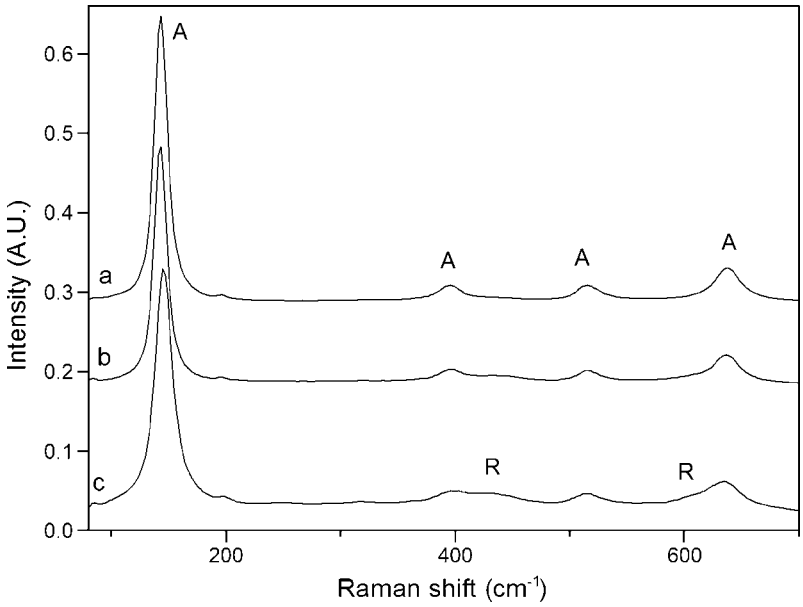

Figure 2. Raman spectra of the studied materials: TiSnT1 (a), TiSnA1 (b) and TiSnB1 (c) (A, anatase; R, rutile).

(cassiterite) phase. This phase appears when the amorphous solid is not thoroughly washed with CH_2Cl_2 (as in sample TiSnB1) or when non-recrystallized Ph_3SnOH is used in the reaction (as in TiSnA1). The adsorption of organotin compounds on the surface of precipitating amorphous TiO_2 particles in reaction (1) leads to nanocrystalline $Ti_{1-x}Sn_xO_2$ materials, with anatase and rutile phases, after calcination in air.[8] When the amorphous solid is not well washed with CH_2Cl_2, additional Ph_3SnCl is deposited on the solid when the solvent is evaporated, and calcination gives rise to the SnO_2 phase. Indeed, we have calcined Ph_3SnCl in air at 723 K and obtained SnO_2.

In order to determine the origin of the SnO_2 phase in TiSnA1, we attempted to identify the nature of the

Table 2. Structural characteristics of the photocatalysts

Sample	Sn content (mass %)	S_{BET} ($m^2\ g^{-1}$)	Crystalline phases	Particle size (nm)
TiSnT1	11	36	Anatase	29
			Rutile	6
TiSnA1	20	41	Anatase	26
			Rutile	6
			SnO_2	5
TiSnB1	23	36	Anatase	18
			Rutile	9
			SnO_2	9
P25	—	44	Anatase	23
			Rutile	34
SnO_2	79	4	Rutile type	84

insoluble impurity in commercial Ph_3SnOH that gives rise to some turbidity when it is dissolved in CH_2Cl_2. For that reason, we washed with ethanol the insoluble residue of the recrystallization until no more solid was dissolved. After drying in air at room temperature, the impurity was characterized as essentially Ph_2SnO by Raman spectroscopy and elemental analysis. Indeed, Ph_2SnO had been previously reported as an impurity of Ph_3SnOH.[45] Therefore, when non-recrystallized Ph_3SnOH is used in reaction (1), Ph_2SnO is co-deposited with the precipitating amorphous TiO_2 particles and organotin compounds are adsorbed on the surface of both solids. Calcination of Ph_2SnO gives rise to the SnO_2 phase, while calcination of the TiO_2 particles, with adsorbed organotin compounds, gives rise to the anatase and rutile phases of $Ti_{1-x}Sn_xO_2$. In short, an SnO_2 phase appears by calcination of a bulk organotin compound, Ph_3SnCl in the case of a poor washing with CH_2Cl_2 (sample TiSnB1) or Ph_2SnO in the case of non-recrystallized Ph_3SnOH (sample TiSnA1), while calcination of organotin compounds adsorbed on the surface of amorphous TiO_2 particles does not give rise to SnO_2, but to tin-doped TiO_2.

Photocatalytic activity for the oxidation of toluene

Figure 3 plots the toluene conversion rates per unit of catalyst surface (measured after reaching the steady state) for the different catalysts reported in Table 2. As expected, SnO_2 shows no measurable activity because of the inability of the photogenerated electrons to reduce oxygen,[13,14,22] and it has not been included in the figure. Among the tin-containing TiO_2-based catalysts, TiSnB1 (with a SnO_2 phase) and TiSnT1 (without SnO_2) display a high catalytic activity that is similar to that found for P25, the material that is often considered as a benchmark in photocatalysis. Nevertheless, TiSnA1 (also containing an SnO_2 phase) has an outstanding catalytic activity for the photooxidation of toluene in the gas phase with an oxidation rate more than twice as high as that corresponding to P25. It is interesting to note the different behaviour of samples TiSnA1 and TiSnB1, reflecting the importance of the method used to incorporate a SnO_2 phase into the final material. Bearing in mind that the photocatalytic oxidation of aromatic compounds is slow in comparison to other organic compounds, and better catalysts are required for the degradation of this kind of pollutants, TiSnA1 is a very promising material and further studies are currently under way.

CONCLUSIONS

The reaction of $TiCl_4$ with Ph_3SnOH in CH_2Cl_2 proceeds to the formation of tin-doped TiO_2 photocatalysts by means of

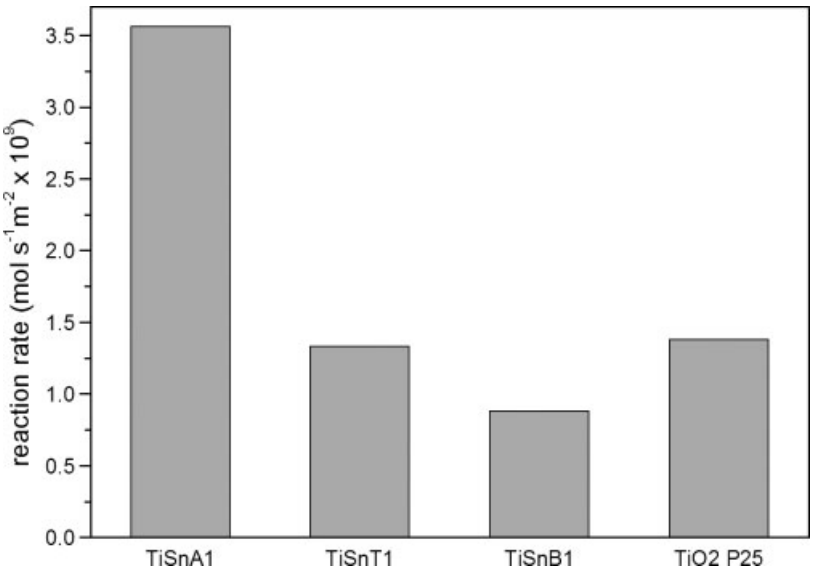

Figure 3. Gas phase toluene degradation rate after reaching the steady state for the studied photocatalysts.

dehydration of Ph_3SnOH and hydrolysis of $TiCl_4$ to amorphous TiO_2 that contains adsorbed organotin compounds and gives rise to the final materials by calcination in air at 723 K. The tin-doped photocatalysts contain the anatase and rutile phases, but not a segregated SnO_2 phase, unless the amorphous precipitate is not thoroughly washed with CH_2Cl_2 or non-recrystallized Ph_3SnOH is used in the reaction. A material that contains a SnO_2 phase, in addition to anatase and rutile, and displays a surprisingly high catalytic activity for the photooxidation of toluene in the gas phase is obtained from non-recrystallized Ph_3SnOH that contains Ph_2SnO.

Acknowledgements

The authors are grateful to the Spanish Ministerio de Educación y Ciencia for financial support (project CTQ2004-03409/BQU) and the award of a doctoral grant to F.F.

REFERENCES

1. Murphy EF, Murugavel R, Roesky HW. *Chem. Rev.* 1997; **97**: 3425.
2. Jagirdar BR, Murphy EF, Roesky HW. *Prog. Inorg. Chem.* 1999; **48**: 351.
3. Roesky HW. *Inorg. Chem.* 1999; **38**: 5934.
4. Honnick WD, Zuckerman JJ. *Inorg. Chem.* 1976; **15**: 3034.
5. Du Mont WW, Neudert B. *Angew. Chem. Int. Edn Engl.* 1980; **19**: 553.
6. Obrey SJ, Barron AR. *J. Chem. Soc. Dalton Trans.* 2001; 2456.
7. Navio JA, Cerrillos C, Pradera MA, Morales E, Gómez-Ariza JL. *Langmuir* 1998; **14**: 388.
8. Fresno F, Coronado JM, Tudela D, Soria J. *Appl. Catal. B: Environ.* 2005; **55**: 159.
9. Fresno F, Guillard C, Coronado JM, Chovelon JM, Tudela D, Soria J, Herrmann JM. *J. Photochem. Photobiol. A: Chem* 2005; **173**: 13.
10. Hoffman MR, Martin ST, Choi W, Bahnemann DW. *Chem. Rev.* 1995; **95**: 69.
11. Linsebigler AL, Lu G, Yates JT. *Chem. Rev.* 1995; **95**: 735.
12. Kawahara T, Konishi Y, Tada H, Tohge N, Nishii J, Ito S. *Angew. Chem. Int. Edn* 2002; **41**: 2811.
13. Vinodgopal K, Bedja I, Kamat PV. *Chem. Mater.* 1996; **8**: 2180.
14. Shi L, Li C, Gu H, Fang D. *Mater. Chem. Phys.* 2000; **62**: 62.
15. Cao Y, Zhang X, Yang W, Du H, Bai Y, Li T, Yao J. *Chem. Mater.* 2000; **12**: 3445.
16. Tada H, Hattori A, Tokihisa Y, Imai K, Tohge N, Ito S. *J. Phys. Chem. B* 2000; **104**: 4585.
17. Kawahara T, Konishi Y, Tada H, Tohge N, Ito S. *Langmuir* 2001; **17**: 7442.
18. Liu Q, Wu X, Wang B, Liu Q. *Mater. Res. Bull.* 2002; **37**: 2255.
19. Pilkenton S, Raftery D. *Solid State Nucl. Magn. Reson.* 2003; **24**: 236.
20. Kanai N, Nuida T, Ueta K, Hashimoto K, Watanabe T, Ohsaki H. *Vacuum* 2004; **74**: 723.
21. Shang J, Yao W, Zhu Y, Wu N. *Appl. Catal. A: Gen.* 2004; **257**: 25.
22. Lin J, Yu JC, Lo D, Lam SK. *J. Catal.* 1999; **183**: 368.
23. Zheng SK, Wang TM, Hao WC, Shen R. *Vacuum* 2002; **65**: 155.
24. Yang J, Li D, Wang X, Yang X, Lu L. *J. Solid State Chem.* 2002; **165**: 193.
25. Davies AG. *Organotin Chemistry*, 2nd edn. Wiley-VCH: Weinheim, 2004.
26. McFarlane W, Wood RJ. *J. Organomet. Chem.* 1972; **40**: C17.
27. Holeček J, Nádvorník M, Handlíř K, Lyčka A. *J. Organomet. Chem.* 1983; **241**: 177.
28. Lockhart TP, Manders WF, Brinckman FE. *J. Organomet. Chem.* 1985; **286**: 153.
29. Kerschl S, Wrackmeyer B, Männig D, Nöth H, Staudigl R. *Z. Naturforsch.* 1987; **42b**: 387.
30. Wharf I, Lamparski H, Reeleder R. *Appl. Organomet. Chem.* 1997; **11**: 969.
31. Maira AJ, Yeung KL, Soria J, Coronado JM, Belver C, Lee CY, Augugliaro V. *Appl. Catal. B: Environ.* 2001; **29**: 327.
32. Fuerte A, Hernández-Alonso MD, Maira AJ, Martínez-Arias A, Fernández-García M, Conesa JC, Soria J, Munuera G. *J. Catal.* 2002; **212**: 1.
33. Friebe E, Kelker H. *Z. Anal. Chem.* 1963; **192**: 267.
34. Wharf I. *Spectrochim. Acta, Pt A.* 1994; **50A**: 903.
35. Harris RK, Sebald A. *Magn. Reson. Chem.* 1989; **27**: 81.
36. Glidewell C, Liles DC. *Acta Crystallogr. Sect. B* 1978; **34**: 129.
37. Glidewell C, Low JN, Bomfim JAS, Filgueiras CAL, Wardell JL. *Acta Crystallogr. Sect. C* 2002; **58**: m199.
38. Harris RK, Reams P, Packer KJ. *J. Mol. Struct.* 1986; **141**: 13.
39. Lockhart TP, Puff H, Schuh W, Reuter H, Mitchell TN. *J. Organomet. Chem.* 1989; **366**: 61.
40. Glidewell C, Liles DC. *Acta Crystallogr. Sect. B* 1978; **34**: 1693.
41. Kriegsmann H, Geissler H. *Z. Anorg. Allg. Chem.* 1963; **323**: 170.
42. Wharf I, Lebuis AM, Roper GA. *Inorg. Chim. Acta* 1999; **294**: 224.
43. Wharf I. *Appl. Organomet. Chem.* 2000; **14**: 39.
44. Oliveira MM, Schnitzler DC, Zarbin AJG. *Chem. Mater.* 2003; **15**: 1903.
45. West R, Baney RH, Powell DL. *J. Am. Chem. Soc.* 1960; **82**: 6269.